

Inclined to splash: triggering and inhibiting a splash with tangential velocity

James C Bird, Scott S H Tsai and Howard A Stone¹

School of Engineering and Applied Sciences, Harvard University,
Cambridge, MA 02138, USA

E-mail: has@seas.harvard.edu

New Journal of Physics **11** (2009) 063017 (10pp)

Received 5 March 2009

Published 12 June 2009

Online at <http://www.njp.org/>

doi:10.1088/1367-2630/11/6/063017

Abstract. When a liquid drop impacts a smooth, solid, dry surface, the drop forms a radially spreading lamella, which can lead to a splash. Previous studies have focused almost exclusively on impacts perpendicular to a surface; yet it is common for drops to impact on angled or moving surfaces. The asymmetry of such impacts leads to an azimuthal variation of the ejected rim, and under certain conditions only part of the rim breaks up to form droplets. We show that the tangential component of impact can act to enhance or suppress a splash. We develop a new model to predict when this type of splashing will occur. The model accounts for our observations of the effects of tangential velocity and agrees well with previous experimental data.

Contents

1. Introduction	2
2. Experiments for the splashing threshold	2
3. A model for splashing with tangential boundary motion	4
4. Comparison of experiments and our model	7
5. Discussion and conclusion	7
Acknowledgments	9
References	9

¹ Author to whom any correspondence should be addressed.

1. Introduction

Upon impact, liquid drops can rapidly spread, splash, or bounce. Splashing remains the least understood of these three responses, in part because there are numerous ways in which drops can break apart [1]–[3]. Here we focus on the impact of drops on smooth surfaces that are rigid and dry. For these conditions, splashing occurs when the rim of the spreading drop becomes airborne, often forming a corona (figure 1). Capillarity subsequently disintegrates the airborne film into satellite droplets, which are crucial to atomization, but are often detrimental in coating processes, such as ink jet printing and pesticide delivery [2]. Most studies of splashing have focused on the impact of drops perpendicular to stationary surfaces [1, 2]. Nevertheless, in many applications, the target surface is either moving relative to the drop, such as raster printing, or inclined, such as leaves on a tree [4]. In this paper, we investigate experimentally and via modeling, how tangential velocity affects splashing on a dry, smooth surface.

The transition from spreading (figure 1(a)) to splashing (figure 1(d)) is often referred to as the splashing threshold. Below the splashing threshold, a radial jet, or lamella, rapidly spreads along the dry surface. Above the threshold, the lamella lifts off of the surface, often within the first observable instances, and breaks into satellite droplets. Even though images of splashing on dry surfaces appear similar to images of splashing on pre-wet surfaces, the dynamics between these two conditions are fundamentally distinct, in part due to the existence of a contact line where the solid, liquid and surrounding gas meet. Therefore, proposed mechanisms for splashing on pre-wet surfaces, such as the propagation of kinematic discontinuities [5], are rarely applicable to initially dry surfaces without additional assumptions.

The splashing threshold on dry surfaces has been shown to depend on the surface roughness [6, 7], the properties of the surrounding gas [8], and the compliance of the solid substrate [9]. Past experiments have found that the splashing threshold follows the empirical relation $We Re^{1/2} = K$, where K is a constant that depends on external parameters such as surface roughness [6, 10]. Here, the Weber and Reynolds numbers are defined as $We = \frac{\rho V^2 R}{\gamma}$ and $Re = \frac{VR}{\nu}$, respectively, where V is the impact velocity of the drop, R is the drop radius, ρ is the liquid density, γ is the surface tension and ν is the kinematic viscosity. While this threshold has been rationalized using theoretical arguments [2, 11, 12], few of these theoretical arguments easily generalize to account for tangential velocity.

Although numerous studies have documented the effects of tangential velocity on drop impact [13]–[18], only a few have reported the effects on splashing on dry surfaces. These experiments have concluded that on an incline, the splashing threshold follows the familiar form, $We Re^{1/2} = K$, provided that the impact velocity is replaced with the normal velocity [6, 10]. Significant tangential velocity can also lead to asymmetric splashing, a phenomenon in which one side of the drop spreads and the other splashes [19]. Here, we quantify the asymmetric splashing behavior and, by treating the sides of the drop separately, develop a physical model that not only agrees well with our experimental data, but also provides insight into the early time dynamics of splashing.

2. Experiments for the splashing threshold

We experimentally measure the impact dynamics of millimeter-sized ethanol drops ($\rho = 790 \text{ kg m}^{-3}$, $\nu = 1.2 \times 10^{-6} \text{ m}^2 \text{ s}^{-1}$ and $\gamma = 23 \text{ mN m}^{-1}$) on to a dry, smooth, aluminum surface. Drops are released from a syringe located between 3 and 67 cm above the surface. The drop

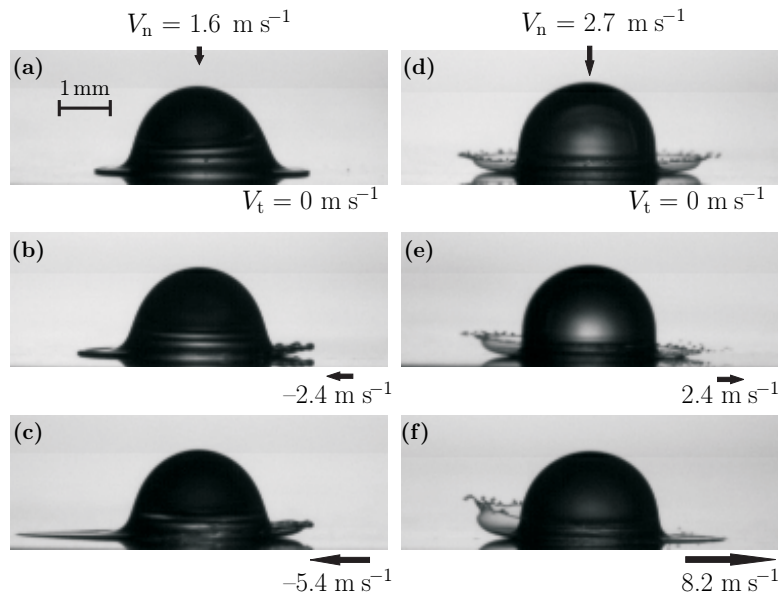


Figure 1. A component of velocity tangent to the surface can both induce and suppress splashing. Arrows indicate the direction of motion of the substrate. (a) No splash occurs when a millimeter-sized ethanol drop impacts normally at 1.2 m s^{-1} upon a flat and stationary aluminum disk. (b) As the substrate moves tangentially (here 2.4 m s^{-1}), the portion of the lamella moving opposite the substrate begins to splash. (c) At even higher tangential velocity (5.4 m s^{-1}) an asymmetric corona splash develops. (d) Above the splashing threshold, increased tangential velocity can act to reduce (e) and eventually suppress (f) a portion of the splash. Images (a)–(c) and (d)–(f) were captured, respectively, 1.3 and 0.5 ms after impact.

size, impact velocity, and subsequent dynamics are measured using a Phantom V7 high-speed camera recording at 15 000 frames per second. We generate a tangential velocity V_t by either moving or inclining the surface relative to the drop. To move the surface at a uniform velocity, we attach an aluminum disk to an analog-controlled electric motor and rotate it so that the tangential velocity 6 centimeters off-center ranges from 0 to 21 m s^{-1} . For the experiments with a stationary inclined plane, the surface is inclined at angles between 0 and 50° from the horizontal.

We find that below the splashing threshold (figure 1(a)), the ethanol drop spreads across the aluminum surface. When the tangential velocity is increased, the portion of the lamella moving in the same direction as the substrate continues to spread, whereas the portion of the lamella moving opposite to the substrate delaminates and splashes (figures 1(b) and (c)). We refer to this symmetry breaking, when one side of the drop spreads while the other side splashes, as asymmetric splashing. We find similar dynamics above the splashing threshold (figure 1(d)). Increased tangential velocity acts to suppress the splash from the lamella moving in the same direction as the applied tangential velocity (figures 1(e) and (f)).

The impact dynamics were similar for both the inclined and moving surfaces for a given normal and tangential velocity. A phase plot of the splashing threshold quantitatively

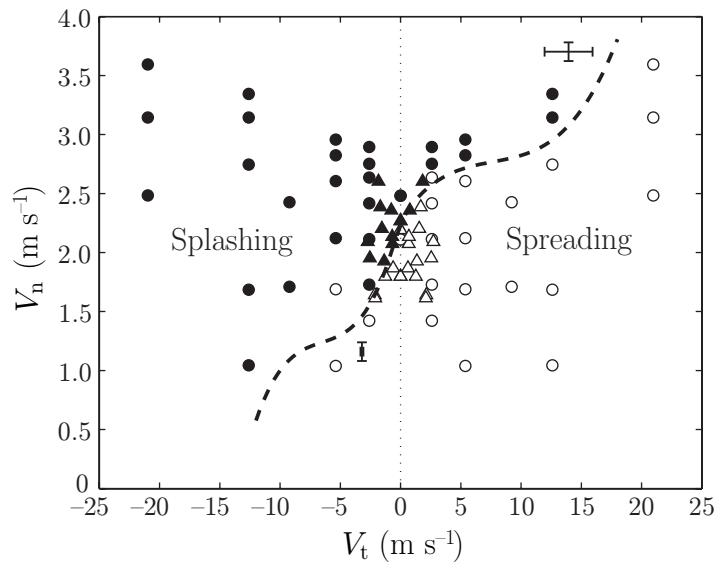


Figure 2. For a given normal drop velocity V_n , increasing the tangential velocity towards the lamella (negative V_t) instigates splashing, causing a spreading lamella (\circ , Δ) to lift off the surface (\bullet , \blacktriangle). Similarly, increasing the tangential velocity away from the lamella (positive V_t) inhibits splashing. The symbols denote whether the surface is moving (\circ , \bullet) or inclined (Δ , \blacktriangle). Here the radius of the drops are $R = 0.88$ mm and the dashed line is a guide for the eye. Representative error bars indicate the size of the 95% confidence intervals at two locations; as the tangential velocity strongly depends on where the drop impacts the disk, the uncertainty increases with both disk speed and drop height.

demonstrates the effects of the tangential velocity (figure 2). Our results agree with previous observations that there is a critical velocity separating spreading and splashing along $V_t = 0$. Additionally, the data quantify how the splashing threshold changes with tangential velocity. When each drop impacts the substrate, we record both the dynamics of the lamella toward ($V_t > 0$) and away ($V_t < 0$) from the direction of the substrate motion. This characterization is responsible for the symmetry in the position of the points in figure 2.

Special attention should be given to the range of tangential velocities needed to significantly influence the splashing threshold. For example, shock waves in the liquid have been shown to be important in lamellar formation [20], though at much higher impact speeds than utilized here. More recently, experiments and theory have linked splashing to the compressibility of the surrounding gas at early times [8, 21]. Nevertheless, the results in figure 2 demonstrate that tangential velocities well below the speed of sound in both liquid and gas are able to have a significant influence on the splashing behavior: the lamella speed traveling tens of meters per second, rather than hundreds of meters per second, affects the splashing threshold. The implication is that the mechanisms responsible for splashing in our study occur when the lamella is traveling on the order of tens of meters per second.

3. A model for splashing with tangential boundary motion

While there exist several models for splashing, these models do not easily generalize to account for tangential velocity. Additionally, the existing models that have been proposed for the

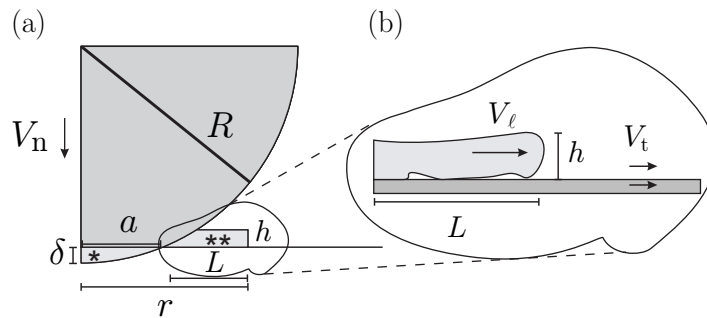


Figure 3. (a) At early times, we assume that the portion of drop (dark gray) that has not contacted the rigid solid is unperturbed and translates at constant velocity V_n . The portion of the drop that has contacted the rigid solid (region *) is redistributed into a lamella around the drop with length L and thickness h (region **). (b) We model the lamella moving outward on a moving surface. In our model, we assume that the important parameters are the bulk lamella velocity V_ℓ , the velocity of the surface and surrounding boundary layer V_t , the lamella thickness h and length L .

early time lamella dynamics, are either not appropriate for dry surfaces [11] or atmospheric pressures [8]. Therefore, instead of generalizing an existing approach, we now introduce a model of the lamella dynamics that builds on ideas from previous studies. The model is based upon our observations that the mechanism behind splashing depends on the dynamics of the lamella relative to the target surface or the surrounding air rather than the dynamics relative to the drop. We describe the lamella with a characteristic length along the flow direction L , thickness h and velocity V_ℓ . In addition, we model the surrounding substrate and gas as moving with velocity V_t (figure 3). All parameters have positive values except for V_t , which is positive when the substrate moves in the same direction as the lamella and negative when the substrate moves in the opposite direction. The air boundary layer over the spinning plate is estimated using the kinematic viscosity of air $\nu = 1.5 \times 10^{-5} \text{ m}^2 \text{ s}^{-1}$ and the maximum angular velocity of the plate $\omega = 5000 \text{ rpm}$. As the thickness of this boundary layer $\sqrt{\nu/\omega} > 400 \mu\text{m}$ is much larger than the initial lamella thickness $h < 50 \mu\text{m}$, we assume that the surrounding solid and gas are moving at the same speed.

Similar to previous models [2, 5, 11, 12], we believe that any instabilities in the film will be described by inertial dynamics. As the inertia of the film relative to the substrate increases, the film may destabilize, overshoot small changes in the surface topography, and become airborne [22]. At the same time, these instabilities are regulated by capillarity. In other words, film deformations caused by substrate or gas-related perturbations increase the interfacial surface area. Only when the kinetic energy of the film relative to the surroundings is much greater than the surface energy preventing deformations will the film become unstable and lead to a splash. In our model, the kinetic energy of the lamella relative to the surroundings scales as $\rho(V_\ell - V_t)^2 L^2 h$ (see figure 3). Similarly, the increase in surface energy due to deformation scales as $\gamma h L$. For splashing to occur, the kinetic energy must be much greater than the change in surface energy, or

$$\frac{\rho(V_\ell - V_t)^2 L^2 h}{\gamma} > C \gg 1, \quad (1)$$

where the value of C depends on the properties of the surroundings. The focus of our model is on the liquid; since we do not consider variations to the solid or surrounding gas, C is a constant much greater than one. Nonetheless, we expect that any additional effects that increase the deformation of the lamella, such as surface roughness or atmospheric pressure, would decrease C .

It is generally apparent whether or not a drop will splash as soon as the lamella is visible, as small perturbations are observable in a destabilized lamella. For a 1 mm radius drop of ethanol with an impact velocity of 2 m s^{-1} , the lamella first appears at about $10 \mu\text{s}$ [9]. The lamella interactions occur so rapidly after contact that accurate measurements of the lamella dimensions and speed are currently limited by the spatial and temporal resolution of high-speed cameras. Instead, we estimate V_ℓ , h and L from the initial conditions of drop impact.

It is typical to model the lamella size and velocity based on a redistribution of fluid due to geometric constraints (figure 3(a)) [8, 11, 23]. In this approach all of the fluid in the drop is assumed to be moving at the speed V_n toward the surface. Once fluid particles contact the rigid surface, they are redistributed outward into the lamella. The consequence is that the volume of the perturbed fluid (region * in figure 3(a)) is equal to the volume of the lamella (region ** in figure 3(a)). Equating the volume of the spherical cap to the volume of the annular disk in figure 3, we find that $\frac{\pi}{6}\delta(3a^2 + \delta^2) = \pi(r^2 - a^2)h$.

The rate at which fluid is displaced depends on the drop speed such that $\delta = V_n t$ and $a \approx \sqrt{2V_n R t}$ near the point of contact, where t is the time since impact. We assume that at very early times the lamella thickness scales proportional to the momentum boundary layer thickness in the liquid, such that $h = c_1 \sqrt{\nu t}$ where c_1 is a scaling constant of ord(1) (e.g. [5, 8, 11]); recent experiments by de Ruiter *et al* (manuscript in review) suggest that the dynamics, while approximately represented by this formula, are more complex. Using these results, we can express the radial extent of the lamella as

$$r = \sqrt{2V_n R t + \frac{V_n^2 R t^2}{c_1 \sqrt{\nu t}} + O((V_n t)^2)}. \quad (2)$$

We see that in the limit that $t \rightarrow 0$, $r \approx \sqrt{V_n R t}$ and $V_\ell = \dot{r} \approx \sqrt{\frac{R V_n}{t}}$, where a dot denotes the time derivative. The difficulty with the limit $t \rightarrow 0$ is that the parameters in which we are interested are no longer finite. One approach to this problem is to regularize the singularity and produce a splashing model that is independent of time (e.g. [8]). Another approach is to note that many of the physical assumptions break down at early times, leading to the significance of such effects as compressibility of the liquid [20, 24] and the role of the intervening gas film [21].

Here, we assume instead that the destabilization process requires that the lamella evolves to be distinctly separate from the drop. Provided that the contact point of the drop $a(t)$ moves faster than the lamella separates from the drop $L(t)$ (figure 3(a)), any destabilization will be engulfed in the drop. It is only when L grows at the same rate or faster than a that we have a distinct lamella. Recalling that $r = L(t) + a(t)$ and $a^2 = 2Rt$, we can see from (2) that $L(t_c) \approx a(t_c)$ at the time

$$t_c \approx \frac{\nu}{V_n^2}. \quad (3)$$

Equation (3), based on the assumed viscous dependence in (2), predicts that for an ethanol drop falling at 1 m s^{-1} , there would be a distinct lamella on the order of $1 \mu\text{s}$ after contact. This estimate is consistent with previous measurements [9]. Since both L and V_ℓ depend on time,

the splashing criterion (1) should depend on time as well. The left-hand side of (1) decreases with time, therefore our model predicts that splashing occurs at the earliest time physically appropriate, which is on the order of t_c . This consequence of the model is also consistent with experiments, which show that splashing develops when the lamella is first observable [8, 9]. At t_c our model predicts the lamellar length and velocity to be

$$L(t_c) \sim \sqrt{V_n R t_c} = c_2 R R e^{-1/2}, \quad (4a)$$

$$V_\ell(t_c) \sim \dot{L} = c_3 V_n R e^{1/2}, \quad (4b)$$

where the Reynolds number $Re = \frac{V_n R}{\nu}$ and c_2 and c_3 are scaling constants of order one.

Substituting the scaling relations for L and V_ℓ into (1), the splashing threshold expression can be re-expressed as

$$We Re^{1/2} \left(1 - k \frac{V_t}{V_n} Re^{-1/2} \right)^2 > K, \quad (5)$$

where the Weber number $We = \frac{\rho V_n^2 R}{\gamma}$, $K = \frac{C}{c_2 c_3^2}$ and $k = 1/c_3$. We expect k to be order one and K to be much greater than one; K has been previously reported to be between 1180 and 19 200 for various, relatively smooth surfaces [6, 10].

4. Comparison of experiments and our model

In the case that the substrate is stationary and flat, $\frac{V_t}{V_n} = 0$, we predict that splashing will occur when $We Re^{1/2} > K$, a result that is consistent with previous splashing data [6, 10]. In these past experiments K has been shown to decrease with surface roughness. We would expect a similar qualitative behavior in our model as well, although the functional form is beyond the scope of this paper.

Our approach makes testable predictions for the splashing behavior when the surface is either inclined or moving relative to the drop trajectory. In figure 4, we plot our experimental results for three sizes of drops following the scaling suggested by equation (5). Specifically, we nondimensionalize the horizontal axis as $(V_t/V_n) Re^{-1/2}$, and the vertical axis as $We Re^{1/2}/K$. With this scaling, the data points, which correspond to whether or not a drop splashed, collapse into distinct regions independent of the drop size. The model prediction agrees well with the experimental data with $k = 2.5$ and $K = 5700$ (solid line in figure 4), values that are consistent with the model (k is ord(1) and $K \gg 1$) and previous experiments [6, 10].

5. Discussion and conclusion

When one side of the drop encounters a positive tangential velocity, the other side of the drop encounters an equal but negative tangential velocity. Therefore, it is natural to inquire how the drop behaves globally in the presence of tangential velocity from any direction. Based on the magnitude of the tangential velocity, there are three behaviors: the lamella will spread in all directions, splash in all directions, or asymmetrically splash (figure 5). As expected, when there is no tangential velocity, the drops either spread or splash in all directions. However, when the

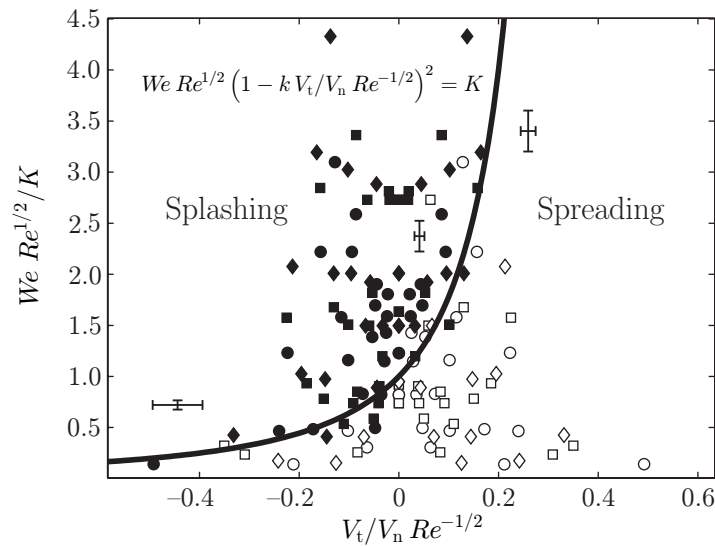


Figure 4. Experimental results for ethanol drops with different radii, $R = 0.88$ mm (\circ , \bullet), 1.3 mm (\square , \blacksquare) and 1.7 mm (\diamond , \blacklozenge), approximately collapse on to a master curve when rescaled according to our theory. The model prediction (solid line) agrees well with the experimental data when $k = 2.5$ and $K = 5700$ in equation (5). Representative error bars are placed at three locations.

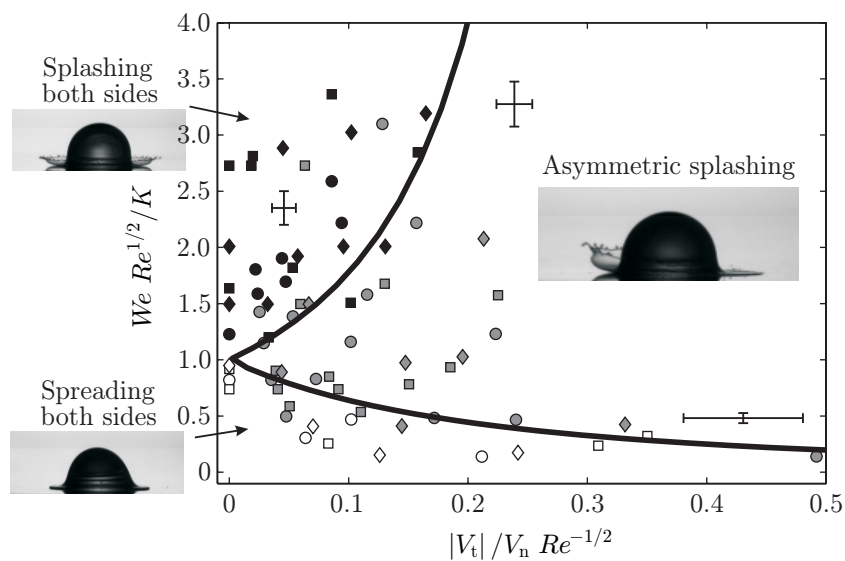


Figure 5. Experimental results from figure 4 recast to show global drop behavior. The model predicts three behaviors based on the magnitude of the tangential velocity: the lamella will spread in all directions (white symbols), splash in all directions (black symbols) or asymmetrically splash (gray symbols). Here $K = 5700$.

symmetry is broken through the tangential velocity, the transition bifurcates to create a new behavior: asymmetric splashing.

In this paper, we have documented the effect of tangential velocity on drop splashing. The experiments demonstrate that sufficient tangential velocity can either trigger or inhibit splashing on a portion of the drop. We develop a physical mechanism for splashing based on the rate of growth of the lamella. Predictions from the model agree well with the experimental observations. These findings are not only relevant to drop impact on moving and inclined surfaces, but also provide insight into the fundamentals of splashing.

Acknowledgments

We thank M Brenner, L Courbin and R Pepper for helpful discussions. We also thank the NSF via the Harvard MRSEC (DMR-0820484) for support of this research.

References

- [1] Rein M 1993 Phenomena of liquid-drop impact on solid and liquid surfaces *Fluid Dyn. Res.* **12** 61–93
- [2] Yarin A L 2006 Drop impact dynamics: splashing, spreading, receding, bouncing *Annu. Rev. Fluid Mech.* **38** 159–92
- [3] Deegan R D, Brunet P and Eggers J 2008 Complexities of splashing *Nonlinearity* **21** C1
- [4] Butterworth J and McCartney H A 1991 The dispersal of bacteria from leaf surfaces by water splash *J. Appl. Bact.* **71** 484–96
- [5] Yarin A L and Weiss D A 1995 Impact of drops on solid-surfaces—self-similar capillary waves and splashing as a new-type of kinematic discontinuity *J. Fluid Mech.* **283** 141–73
- [6] Stow C D and Hadfield M G 1981 An experimental investigation of fluid-flow resulting from the impact of a water drop with an unyielding dry surface *Proc. R. Soc. A* **373** 419–41
- [7] Range K and Feuillebois F 1998 Influence of surface roughness on liquid drop impact *J. Colloid Interface Sci.* **203** 16–30
- [8] Xu L, Zhang W W and Nagel S R 2005 Drop splashing on a dry smooth surface *Phys. Rev. Lett.* **94** 184505
- [9] Pepper R E, Courbin L and Stone H A 2008 Splashing on elastic membranes: the importance of early-time dynamics *Phys. Fluids* **20** 082103
- [10] Mundo C, Sommerfeld M and Tropea C 1995 Droplet–wall collisions—experimental studies of the deformation and breakup process *Int. J. Multiph. Flow* **21** 151–73
- [11] Josserand C and Zaleski S 2003 Droplet splashing on a thin liquid film *Phys. Fluids* **15** 1650–7
- [12] Roisman I V, Horvat K and Tropea C 2006 Spray impact: rim transverse instability initiating fingering and splash and description of a secondary spray *Phys. Fluids* **18** 102104
- [13] Yao S and Cai K Y 1988 The dynamics and leidenfrost temperature of drops impacting on a hot surface at small angles *Exp. Therm. Fluid Sci.* **1** 363–71
- [14] Bussmann M, Mostaghimi J and Chandra S 1999 On a three-dimensional volume tracking model of droplet impact *Phys. Fluids* **11** 1406–17
- [15] Roisman I V and Tropea C 2002 Impact of a drop onto a wetted wall: description of crown formation and propagation *J. Fluid Mech.* **472** 373–97
- [16] Sikalo S, Tropea C and Ganic E N 2005 Impact of droplets onto inclined surfaces *J. Colloid Interface Sci.* **286** 661–9
- [17] Chen R H and Wang H W 2005 Effects of tangential speed on low-normal-speed liquid drop impact on a non-wettable solid surface *Exp. Fluids* **39** 754–60

- [18] Moreira A L N, Moita A S, Cossali E, Marengo M and Santini M 2007 Secondary atomization of water and isooctane drops impinging on tilted heated surfaces *Exp. Fluids* **43** 297–313
- [19] Courbin L, Bird J C and Stone H A 2006 Splash and anti-splash: observation and design *Chaos* **16** 041102
- [20] Dear J P and Field J E 1988 High-speed photography of surface geometry-effects in liquid solid impact *J. Appl. Phys.* **63** 1015–21
- [21] Mandre S, Mani M and Brenner M P 2009 Precursors to splashing of liquid droplets on a solid surface *Phys. Rev. Lett.* **102** 134502
- [22] Josserand C, Lemoyne L, Troeger R and Zaleski S 2005 Droplet impact on a dry surface: triggering the splash with a small obstacle *J. Fluid Mech.* **524** 47–56
- [23] Kim H Y, Feng Z C and Chun J H 2000 Instability of a liquid jet emerging from a droplet upon collision with a solid surface *Phys. Fluids* **12** 531–41
- [24] Field J E, Dear J P and Ogren J E 1989 The effects of target compliance on liquid-drop impact *J. Appl. Phys.* **65** 533–40